Giardia duodenalis induces paracellular bacterial translocation and causes postinfectious visceral hypersensitivity

Marie C M Halliez, Jean-Paul Motta, Troy D Feener, Gaëtan Guerin, Laetitia Legoff, Arnaud François, Elodie Colasse, Loic Favennec, Gilles Gargala, Tamia K Lapointe, et al.

Am J Physiol Gastrointest Liver Physiol 310: G574–G585, 2016.
First published January 7, 2016; doi:10.1152/ajpgi.00144.2015.

Giardia duodenalis induces paracellular bacterial translocation and causes postinfectious visceral hypersensitivity

Marie C. M. Halliez,[1,2] Jean-Paul Motta,[2] Troy D. Feener,[2] Gaetan Guérin,[1] Laetitia LeGoff,[1] Arnaud François,[1,3] Elodie Colasse,[3] Loic Favennec,[1] Gilles Gargala,[1] Tamia K. Lapointe,[4] Christophe Altier,[4] and André G. Buret[2]

[1]*Protozooses transmises par l'alimentation, Rouen University Hospital, University of Rouen and University of Reims Champagne-Ardennes, and Institute for Biomedical Research, Rouen and Reims, France;* [2]*Department of Biological Sciences, Inflammation Research Network, Host-Parasite Interaction NSERC-CREATE, University of Calgary, Calgary, Alberta, Canada;* [3]*Service d'Anatomie et de Cytologie Pathologique CHU Rouen, Rouen cedex, France; and* [4]*Snyder Institute for Chronic Diseases, Inflammation Research Network, Department of Physiology and Pharmacology, University of Calgary, Calgary, Alberta, Canada*

Submitted 7 May 2015; accepted in final form 4 January 2016

Halliez MC, Motta JP, Feener TD, Guérin G, LeGoff L, François A, Colasse E, Favennec L, Gargala G, Lapointe TK, Altier C, Buret AG. *Giardia duodenalis* induces paracellular bacterial translocation and causes postinfectious visceral hypersensitivity. *Am J Physiol Gastrointest Liver Physiol* 310: G574–G585, 2016. First published January 7, 2016; doi:10.1152/ajpgi.00144.2015.—Irritable bowel syndrome (IBS) is the most frequent functional gastrointestinal disorder. It is characterized by abdominal hypersensitivity, leading to discomfort and pain, as well as altered bowel habits. While it is common for IBS to develop following the resolution of infectious gastroenteritis [then termed postinfectious IBS (PI-IBS)], the mechanisms remain incompletely understood. *Giardia duodenalis* is a cosmopolitan water-borne enteropathogen that causes intestinal malabsorption, diarrhea, and postinfectious complications. Cause-and-effect studies using a human enteropathogen to help investigate the mechanisms of PI-IBS are sorely lacking. In an attempt to establish causality between giardiasis and postinfectious visceral hypersensitivity, this study describes a new model of PI-IBS in neonatal rats infected with *G. duodenalis*. At 50 days postinfection with *G. duodenalis* (assemblage A or B), long after the parasite was cleared, rats developed visceral hypersensitivity to luminal balloon distension in the jejunum and rectum, activation of the nociceptive signaling pathway (increased c-*fos* expression), histological modifications (villus atrophy and crypt hyperplasia), and proliferation of mucosal intraepithelial lymphocytes and mast cells in the jejunum, but not in the rectum. *G. duodenalis* infection also disrupted the intestinal barrier, in vivo and in vitro, which in turn promoted the translocation of commensal bacteria. *Giardia*-induced bacterial paracellular translocation in vitro correlated with degradation of the tight junction proteins occludin and claudin-4. The extensive observations associated with gut hypersensitivity described here demonstrate that, indeed, in this new model of postgiardiasis IBS, alterations to the gut mucosa and c-*fos* are consistent with those associated with PI-IBS and, hence, offer avenues for new mechanistic research in the field.

Giardia; irritable bowel syndrome; visceral hypersensitivity; bacterial translocation; tight junctions

THE INTESTINAL PROTOZOAN PARASITE *Giardia duodenalis* (syn. *G. lamblia*, *G. intestinalis*) infects a wide array of mammalian species, including humans. Giardiasis is one of the most common water-borne parasitic infections of the human intestine, and its acute clinical symptoms include intestinal malabsorption and diarrhea (14, 81). The prevalence of giardiasis ranges from 20% to 100% in developing countries and from 3% to 7% in industrialized nations (68). *G. duodenalis* is divided into eight distinct genetic assemblages (i.e., assemblages A–H). While only assemblages A and B are pathogenic to humans, they can also infect nonhuman mammalian species, thus highlighting the zoonotic potential of this parasite (11). The pathophysiology of giardiasis is multifactorial and involves host and parasite factors, as well as immunological and nonimmunological mucosal processes (23). In addition to acute symptoms, *Giardia* infections have also been associated with ocular pathologies, arthritis, failure to thrive, stunting, growth retardation, and cognitive impairment in children (33). Giardiasis can also lead, postinfectiously, to chronic diseases, such as chronic fatigue syndrome and functional gastrointestinal (GI) disorders, via unknown mechanisms (33).

Irritable bowel syndrome (IBS) is the most common functional GI disorder in industrialized countries (41, 51). It is characterized by abdominal pain and discomfort and alteration of bowel habits. IBS manifests in the absence of overt underlying pathology or biomarkers, although low-grade inflammation has been proposed as a contributing factor (15). In some patients, IBS may arise following infectious gastroenteritis (e.g., with *Campylobacter jejuni*, *Escherichia coli*, *Salmonella* spp., or even viral enteritis) (7, 54, 55). Recent studies have also associated protozoan parasites such as *G. duodenalis* or *Cryptosporidium* sp. with the onset of postinfectious IBS (PI-IBS) (35, 46). It is estimated that 7–31% of patients with infectious gastroenteritis go on to develop PI-IBS (34). PI-IBS has also been shown to occur long after clearance of the inciting pathogen. The risk of developing IBS increases sixfold after GI infections and remains elevated for several years after infection, further underscoring the significant potential for these symptoms to occur over the long term (36, 54, 76). Nevertheless, a cause-and-effect relationship has yet to be established experimentally in a model using a human enteropathogen known to cause PI-IBS. Recently, after an outbreak of giardiasis in Bergen, Norway, numerous cases of chronic fatigue and IBS (with diarrheal subtype) and functional dyspepsia were reported in the infected population (35). Several pathophysiological mechanisms, including visceral hypersensitivity (3), central nervous system dysregulation (1), and GI

Address for reprint requests and other correspondence: A. G. Buret, Dept. of Biological Sciences, Inflammation Research Network, Univ. of Calgary, 2500 Univ. Dr. NW, Calgary, AB, Canada T2N 1N4 (e-mail: aburet@ucalgary.ca).

motility abnormalities (9, 45), have been associated with the pathogenesis of IBS. Increased intestinal permeability and changes in microbiota composition have also been reported in some of these patients (43). However, the biological basis of PI-IBS remains incompletely understood.

The aim of the present study was to develop an animal model enabling the demonstration of causality between giardiasis and PI-IBS and to further describe, in this model, abnormalities that have been associated with postinfectious visceral hypersensitivity in humans. In turn, such a model could be used to study postgiardiasis IBS and the underlying mechanisms in its pathogenesis. Using a novel neonatal rat model, we established that infection with *G. duodenalis* assemblage A or B can lead to visceral hypersensitivity in the jejunum, as well as in the rectum, 50 days postinfection (PI), at which time the parasite has been completely cleared from the host. In this model, postinfectious jejunal hypersensitivity was associated with villus atrophy and crypt hyperplasia and increased mucosal intraepithelial lymphocytes (IELs) and mast cells. In contrast, rectal hypersensitivity occurred in the absence of detectable changes in IELs or mast cells. During the acute stage of infection, *Giardia* facilitated the translocation of commensal bacteria and activated the expression of nociceptive c-*fos* in the spinal dorsal horn that received sensory input. Additional mechanistic experiments demonstrated that *Giardia*-induced bacterial translocation was primarily paracellular and implicated disruption of the tight junction proteins occludin and claudin-4.

METHODS AND MATERIALS

G. duodenalis Isolates

Giardia trophozoites were maintained axenically or excysted through passage in gerbils (*Meriones unguculatus*). Two different assemblages (A and B), one isolate per assemblage (WB and H3, respectively), were used.

WB trophozoites [WB; genotype A, catalog no. 30957, American Type Culture Collection (ATCC)-LGC Promochem, Molsheim, France] were maintained in axenic cultures in Keister's modified TYI-S-33 medium (24, 44).

H3 isolates (HB; water-borne, P101, New Orleans, LA, cysts of *G. lamblia*, human isolate H-3, aka CH-3) were obtained by excystation through passage in gerbils. Gerbils were orally infected with a suspension of 10^3 cysts. At 7 days PI, gerbils were euthanized by intraperitoneal injection of a lethal dose of pentobarbitone sodium (Abbott Diagnostic, Rungis, France). After laparotomy, the duodenum and jejunum were sampled, and parasites were extracted, counted, and diluted for infection.

Animal Model Infection

Five-day-old suckling Sprague-Dawley rats and their mother (Janvier, Le Genest Saint Isles, France) were maintained under pathogen-free conditions and given food and water ad libitum. Suckling rats were orally infected with 10^4 live *Giardia* trophozoites in 100 μl of TYI-S-33 medium: 30 rats were infected with WB, and 30 rats were infected with H3. Vehicle-treated animals ($n = 20$) were gavaged with vehicle (100 μl of TYI-S-33 medium). Animals were handled according to the regulations enforced by the French Ministry of Agriculture, the University Ad Hoc Ethical Committee (which aproved the protocol), and the Canadian Council of Animal Care. Rats were studied at 7 days PI (peak of infection), 21 days PI (clearance), and 50 days PI (postinfectious period).

Assessment of Visceral Hypersensitivity to Balloon Distension

Jejunal and rectal sensitivity to balloon distension was tested in 15 rats from each group at 50 days PI, as previously described (46, 57). Sex distribution within the groups was as follows: 9 females and 8 males in the vehicle-treated group, 9 males and 4 females in the WB-infected group, and 14 males and 4 females in the H3-infected group. Rats were anesthetized with pentobarbitone sodium (Pentobarbital Sodique, Ceva Santé Animale, Libourne, France; 6 mg/kg ip). The ventral neck was incised to expose the trachea, in which an incision was made, and a tube was inserted and fixed to allow smooth breathing throughout the experiment. A midline abdominal incision was made to expose the small intestine. At 7 cm from the ligament of Treitz, an incision was made on the antimesenteric side of the jejunum, in which a balloon was inserted and fixed. The intestinal segment was returned to the peritoneal cavity, which was sutured (2-0 Ercylene II, Sherwood Davis & Geck, Bondoufle, France). Rectal distensions were performed by insertion of a balloon via the anal route. Balloons were arterial embolectomy catheters (5F, 10 mm diameter, 80 cm long; Fogarty-Edwards Life Sciences, Saint-Priex, Switzerland). Distensions in the jejunum and rectum were performed in a stepwise fashion (from 0.1 to 0.4 ml and from 0.2 to 1.0 ml, respectively). Twenty-second distensions were followed by a 5-min rest period. Blood pressure variation was continuously recorded from a side-arm carotid cannula with a pressure transducer (model P10EZ, Gould, Courtaboeuf, France) connected to a window graph 240 (Gould), linked to a data acquisition-and-analysis module (iWorx404, Bioseb, Vitrolles, France). All data were recorded and analyzed using LabScribe2 software (Bioseb).

Infection Assessment

At 7 days PI, the presence of *G. duodenalis* trophozoites in the intestine was assessed by microscopic observation, and the infecting assemblage was identified by nested PCR and confirmed by sequencing (data not shown) (29, 47).

Histology

At 7, 21, and 50 days PI, five rats from each group were euthanized by a lethal dose of pentobarbitone sodium (Ceva Santé Animale; 50 mg/kg ip). Sections of the duodenum and jejunum were fixed in 10% formaldehyde solution and embedded in paraffin.

Sections (4 μm) were stained with Giemsa stain for analysis. Villus heights (VH) and crypt depths (CD) were measured on sagittal sections of 15 villus-crypt units using image analysis software (Histolab 6.13.0, Microvision, Evry, France). For each group, the VH-to-CD ratio was calculated as the mean VH divided by the mean CD.

IELs were labeled in 4-μm sections with periodic acid-Schiff staining and counted per villus for 10 villi in each animal.

Mast cells were stained by immunohistochemistry using monoclonal mouse anti-mast cell tryptase antibody (Abcam, Paris, France) and horseradish peroxidase (HRP)-conjugated goat anti-mouse secondary antibody (ultraView Universal DAB Detection Kit, Ventana, Roche, Boulogne-Billancourt, France). Mast cells were counted per villus for 100 villi in each animal.

Assessment of c-fos Expression

At 7, 21, and 50 days PI, in five rats per group, c-*fos* expression was assessed in fresh spinal cord samples by RT-quantitative PCR using a previously validated approach (40). Spinal cord sections between T_{10} and L_2 were frozen in RNAlater (Qiagen) and stored at −70°C until RNA extraction. RNA extractions and reverse transcription were performed on 20 mg of spinal cord following the manufacturer's instructions (RNeasy Mini Kit and QuantiTect Reverse Transcription Kit, Qiagen). Quantitative real-time PCRs were carried out in a thermocycler (Rotor-Gene Q) at 60°C (QuantiFast SYBR Green PCR kit, Qiagen). We used GAPDH as internal control and targeted the

gene c-*fos* (40) (Table 1). Analyses were performed using Rotor-Gene Q software, and the cycle threshold ($2^{-\Delta\Delta C_t}$) method was applied to measure the fold change in mRNA expression between the control and the infected group (70).

Assessment of Bacterial Translocation In Vivo

Plating. Spleen, liver, and mesenteric lymph nodes (MLNs) were aseptically removed and homogenized using two 3.2-mm stainless steel beads (FastPrep-24, MP Biomedical). After homogenization, samples were plated on Columbia agar containing 5% sheep blood for 2 days at 37°C under aerobic or anaerobic conditions [AnaeroGen 2.5L pack in an AnaeroJar (Oxoid, Thermo Scientific)], and colony-forming units (CFUs) were enumerated. Bacterial counts were standardized in CFUs per gram of tissue.

Fluorescence in situ hybridization. Segments of colon were fixed in 4% paraformaldehyde overnight and embedded in paraffin. For fluorescence in situ hybridization (FISH), tissue was hybridized with a universal bacterial 16S fluorescent rRNA probe (EUB338-Cy3, 5′GCTGCCTCCCGTAGGAGT-Cy3, AlphaDNA, Montreal, PQ, Canada) at 10 ng/μl and a control negative probe (NEUB338-Cy3, 5′ACTCCTACGGGAGGCAGC-Cy3, AlphaDNA) at 5 ng/μl and immunostained for DNA by 4′,6-diamidino-2-phenylindole (Sigma-Aldrich). Images were acquired with a Leica DMR fluorescence microscope.

Cell Culture

Caco-2 human colonic epithelial cells (*passages 26–36*, HTB-37, ATCC) were grown in minimum essential medium with 1× Earle's salt (MEME; Sigma-Aldrich, Oakville, ON, Canada) containing 20% fetal bovine serum, 200 mM L-glutamine, 100 U/ml penicillin, 100 U/ml streptomycin, and 100 mM sodium pyruvate and incubated at 37°C and 5% CO_2. For translocation studies, cells were seeded at 10^4 cells/ml onto Transwell filters [12-mm filter with 3.0-μm pore polycarbonate membrane insert (Costar, Corning, NY)]. Transepithelial electrical resistance (TER) was monitored with an electrovoltohmeter (World Precision Instruments, Sarasota, FL), and monolayers were used at confluence (TER >400 Ω). For internalization assay, cells were seeded at 10^4 cells/ml onto flat-bottom plates (BD BioCoat, Becton Dickinson Biosciences, Mississauga, ON, Canada).

Assessment of Bacterial Translocation In Vitro

Monolayers were used in antibiotic-free MEME to the apical and basolateral compartments of the Transwell system. Monolayers were infected apically in the presence or absence of *G. duodenalis* assemblage A at a multiplicity of infection (MOI) of 10^1 trophozoites/enterocyte and in the presence or absence of *E. coli* HB101 at a MOI of 100 CFUs/enterocyte (4 groups: vehicle, *Giardia*, *E. coli*, and *Giardia* + *E. coli*). After 1, 2, 3, and 6 h of incubation in aerobic conditions, *E. coli* recovered in the basolateral compartment were enumerated by spreading serial dilutions onto nonselective Luria broth (LB) agar and aerobic incubation overnight at 37°C.

Assessment of Bacterial Internalization

After coinfection, monolayers were incubated for 1 h with MEME 20% containing gentamicin (250 μg/ml; Sigma-Aldrich) and lysed with RIPA buffer (1% Igepal, 0.1% SDS, and 0.5% sodium deoxycholate in PBS) containing a protease inhibitor (Complete Mini, Roche Diagnostic, Indianapolis, IN; 1 tablet/10 ml). Viable bacteria were enumerated by spreading onto nonselective LB agar. A preliminary experiment confirmed that surface *E. coli* were killed by the gentamicin treatment: for each condition (vehicle, *Giardia*, *E. coli*, and *Giardia* + *E. coli*), serial dilutions of the supernatant after 1 h of incubation with gentamicin were plated on LB agar; no bacteria were observed after 24 h of incubation at 37°C (data not shown).

Immunoblotting of Tight Junction Proteins

Protein concentrations from lysates of cell monolayers were assessed by Bradford assay (DC protein assay kit, Bio-Rad Laboratories, Hercules, CA). Protein concentration was normalized at 3 mg/ml. Samples were diluted 1:1 in 2× Laemmli buffer before Western blotting. Temporary Ponceau red S staining was used to verify the transfer efficiency, as well as the loading, of proteins (67). Membranes were then immunostained for occludin and claudin-4 with rabbit polyclonal anti-claudin-4 antibody (0.2 μg/ml; Abcam) or mouse monoclonal anti-occludin antibody (0.5 μg/ml; Invitrogen) overnight at 4°C under agitation. HRP-conjugated rat anti-rabbit IgG (1:1,000 dilution) in Tris-buffered saline-Tween 20 with 5% dry milk or HRP-conjugated goat anti-mouse IgG (1:1,000 dilution) was used as secondary antibody. Bands were visualized using the ECL Plus Western blotting detection system (GE Healthcare, Pittsburgh, PA).

Statistical Analysis

Values are means ± SE. Comparison between groups was evaluated using *t*-test, Mann-Whitney test, Kruskall-Wallis-Newman test, or one- or two-way ANOVA, depending on the data distribution and experimental setup. $P < 0.05$ at 95% confidence interval was considered significant.

RESULTS

G. duodenalis Induces Visceral Hypersensitivity at 50 Days PI in Immunocompetent Rats

Measurements of visceral hypersensitivity are among the main features of IBS and have been used in models of PI-IBS and postinflammatory IBS (9, 46). For an accurate and reproducible identification of visceral hypersensitivity in animal models, most experts in the field rely on a barostat technique using balloon distension (19). Consistent with this approach, we measured blood pressure upon intraluminal balloon distension, as a drop in cardiovascular pressure is predictive of visceral nociception (50, 69).

At 50 days PI, the drop in blood pressure was significantly increased in assemblage A-infected compared with vehicle-treated rats in response to distension volumes of 0.3 and 0.4 ml in the jejunum (Fig. 1*A*). A similar trend was observed in the rectum at distension volumes of 0.6, 0.8, and 1 ml (Fig. 1*B*). Visceral hypersensitivity was detected in 12 of 19 animals tested (7 of 9 males and 4 of 4 females).

At 50 days PI, the drop in blood pressure was significantly higher in assemblage B-infected than vehicle-treated rats start-

Table 1. *Primer sequences of GAPDH and c*-fos

Target Gene	Sequences		PCR Product Size	Annealing Temperature, °C
	Forward	Reverse		
GAPDH	5′-GGAAAGCTGTGGCGTGATTGG-3′	5′-GTAGGCCATGAGGTCCACCA-3′	414	60
c-*fos*	5′-AACCATCCCCGAAATCCTAC-3′	5′-AGCGGAACAGAGAAACTGGA-3′	185	60

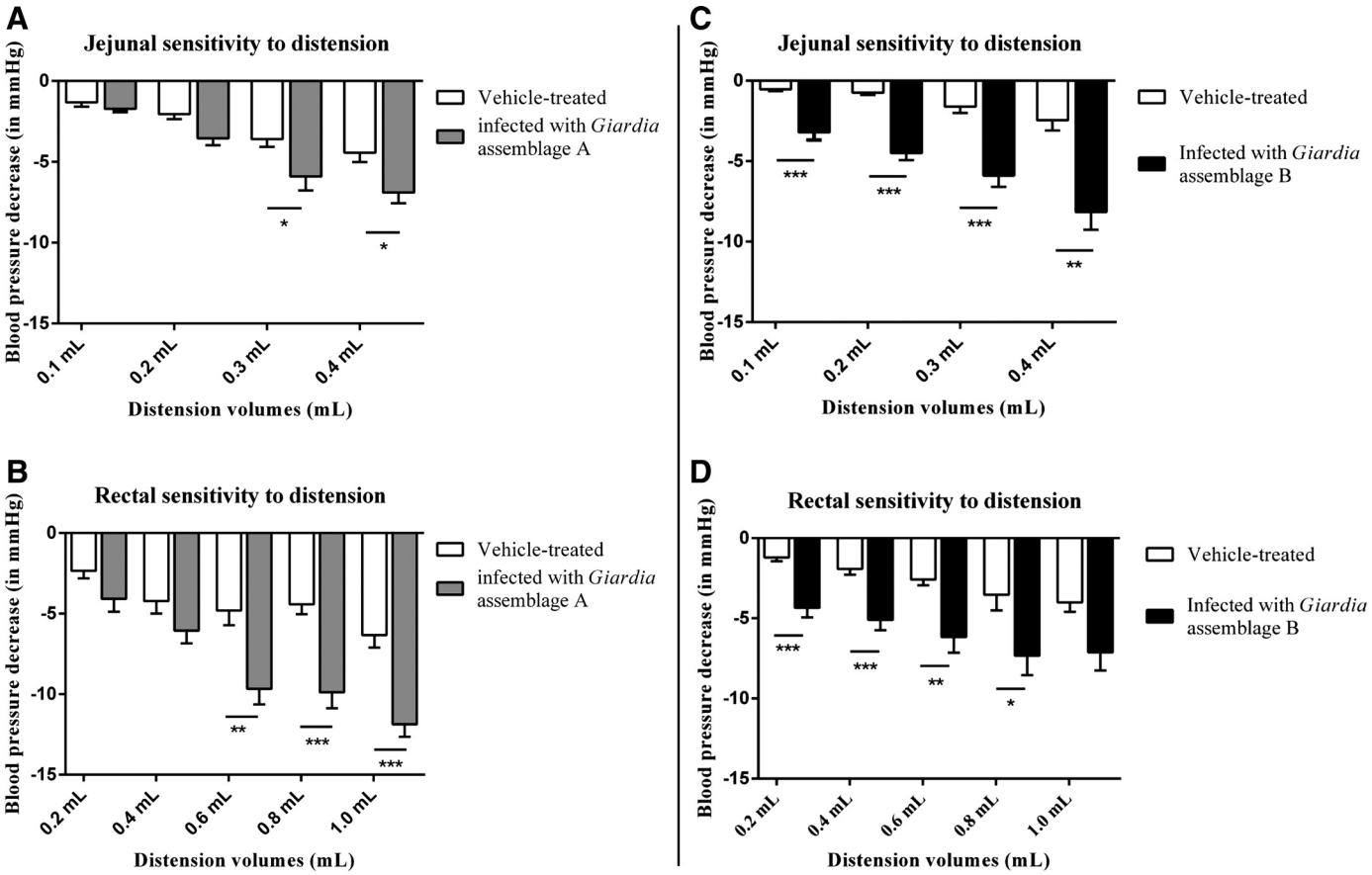

Fig. 1. *Giardia duodenalis* assemblages A and B induce visceral hypersensitivity in the jejunum and rectum at 50 days postinfection (PI): assessment of the decrease in carotid artery blood pressure in control and *Giardia*-infected animals during jejunal and rectal balloon distensions. *A* and *B*: jejunal and rectal sensitivity to distension at 50 days PI using *G. duodenalis* assemblage A (strain WB). *C* and *D*: jejunal and rectal sensitivity to distension at 50 days PI using *G. duodenalis* assemblage B (strain H3). Values are means ± SE ($n = 20$ in each group). *$P < 0.05$, **$P < 0.01$, and ***$P < 0.001$ vs. vehicle-treated (by Student's *t*-test and Newman-Keuls test).

ing at 0.1 ml of distension (Fig. 1*C*). Similarly, in the rectum, the drop in blood pressure was significantly higher in infected than vehicle-treated rats starting at 0.2 ml of distension (Fig. 1*D*). Visceral hypersensitivity was observed in 10 of 18 animals tested (7 of 14 males and 3 of 4 females).

G. duodenalis Infection Induces Modification of the Mucosal Architecture

Several host species have been shown to exhibit intestinal villus atrophy and crypt hyperplasia, as well as microvillus atrophy, in response to giardiasis (13, 14). We assessed the mucosal architecture in the duodenum and jejunum of animals at 7, 21, and 50 days PI.

Duodenal villus length of assemblage A- and B-infected rats was reduced at 50 days PI (Fig. 2*A*).

Crypt length was increased in the duodenum of assemblage B-infected rats at 7 and 21 days PI and assemblage A-infected rats at 21 days PI compared with vehicle-treated rats (Fig. 2*B*). Overall villus-to-crypt ratios in the duodenum remained unchanged at each time point (Fig. 2*C*).

Crypt length in the jejunum of assemblage B-infected rats was increased at 21 days PI (Fig. 2*E*). No other significant changes were observed in the jejunal architecture of assemblage A- and B-infected rats compared with vehicle-treated rats (Fig. 2, *D–F*).

G. duodenalis Increases Mucosal IELs and Mucosal Mast Cells at 50 Days PI in the Jejunum, but not in the Rectum

Colonic mast cell infiltration and degranulation in proximity to mucosal innervations have been suggested as a contributing factor to abdominal pain in IBS (5). IELs have also been shown to be increased in some tissues from patients with IBS, but not in others (74, 78). We assessed mast cell and IEL numbers in the jejunum and rectum of experimental animals. At 50 days PI, a significant increase in IEL and mucosal mast cell numbers was observed in the jejunum of assemblage A- and B-infected compared with vehicle-treated rats (Figs. 3*B* and 4*B*). No significant changes were observed at 7 days PI for either assemblage (Figs. 3*A* and 4*A*). In the rectum, where IEL and mast cell numbers were low, no significant differences were observed upon infection with either *Giardia* assemblage (Figs. 3*C* and 4*C*).

G. duodenalis Infection Induces c-fos Expression in the Spinal Dorsal Horn

The protooncogene c-*fos* is a marker of neuronal activity in the spinal neurons that receive sensory input. Neuronal expression of c-*fos* was shown to be increased in animal models of visceral pain and IBS (82). To further evaluate whether *Giardia* infection could induce the activation of spinal neurons, we assessed c-*fos* mRNA expression in *Giardia*-infected animals.

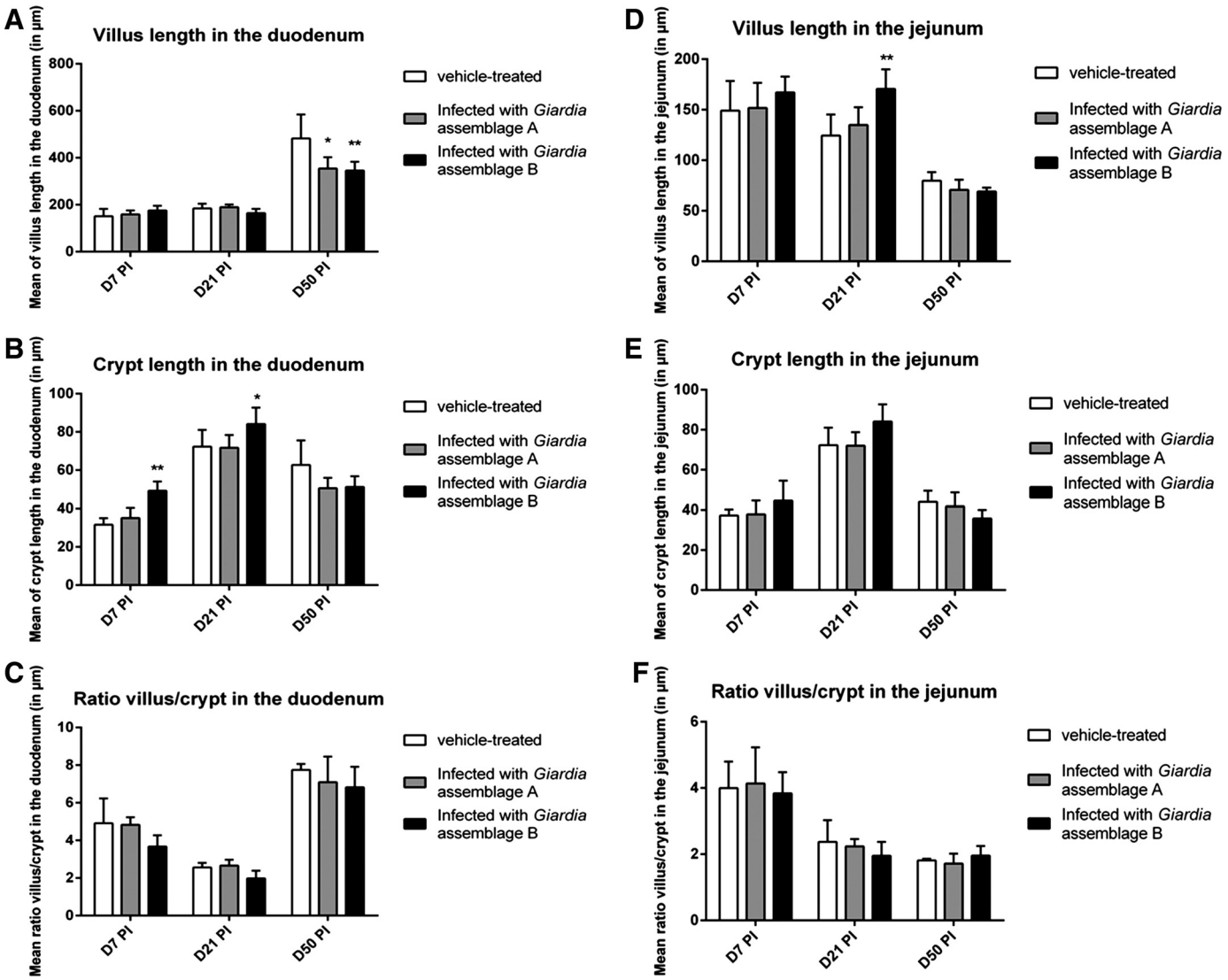

Fig. 2. *Giardia* assemblages A and B induce mucosal architecture modifications in the duodenum and jejunum at 7, 21, and 50 days (D7, D21, and D50) PI: measure of crypt and villus length of the duodenal and jejunal mucosa of vehicle-treated and *Giardia*-infected animals at 7, 21, and 50 days PI after Giemsa staining on 15 well-oriented villus-crypt units. *A* and *B*: average villus and crypt length in the duodenum of rats at 7, 21, and 50 days PI. *C* and *F*: average ratio of villus height to crypt depth in the duodenum and jejunum of rats at 7, 21, and 50 days PI. *D* and *E*: average villus and crypt length in the jejunum of rats at 7, 21, and 50 days PI. Values are means ± SE ($n = 10$ in each group). *$P < 0.05$ and **$P < 0.01$ (by ANOVA and Tukey's test).

At 7, 21, and 50 days PI, the mRNA expression levels of c-*fos* in the spinal cord were significantly increased in assemblage A-infected compared with vehicle-treated rats (Fig. 5).

Giardia Assemblage A Induces Translocation of Commensal Bacteria In Vivo

Microbiota play an important role in health and disease (72), and we recently demonstrated that *Giardia* infection alters the host microbiota at a structural and compositional level (6). In addition, our group previously demonstrated that another enteric pathogen, *C. jejuni*, was able to induce bacterial translocation (42). In an attempt to identify factors that may contribute to the appearance of visceral hypersensitivity, we tested whether *G. duodenalis* could facilitate the translocation of commensal bacteria through the intestinal epithelium during the acute phase of infection.

The present findings illustrate that *Giardia* infection promotes the translocation of commensal bacteria to the spleen and liver at 7 days PI, an effect that was lost at 21 and 50 days PI (Fig. 6).

We observed a thinning of the mucus layer accompanied by bacterial infiltration in our infected animals at 7, 21, and 50 days PI, while the normal colonic structure was maintained in vehicle-treated animals. Although bacterial translocation was not observed in the spleen and liver at 21 and 50 days PI, observations of the colonic mucosal structure showed infiltration maintained at 21 and 50 days PI in the colonic mucosa of *Giardia*-infected rats (Fig. 7).

Giardia Induces Translocation of Noninvasive E. coli Through Caco-2 Monolayers and Tight Junction Protein Degradation

The mechanisms of *Giardia*-induced bacterial translocation were further characterized in Caco-2 cell monolayers grown on Transwell filters. Translocation of *E. coli* HB101 induced by *Giardia* was assessed at 1, 2, 3, and 6 h PI.

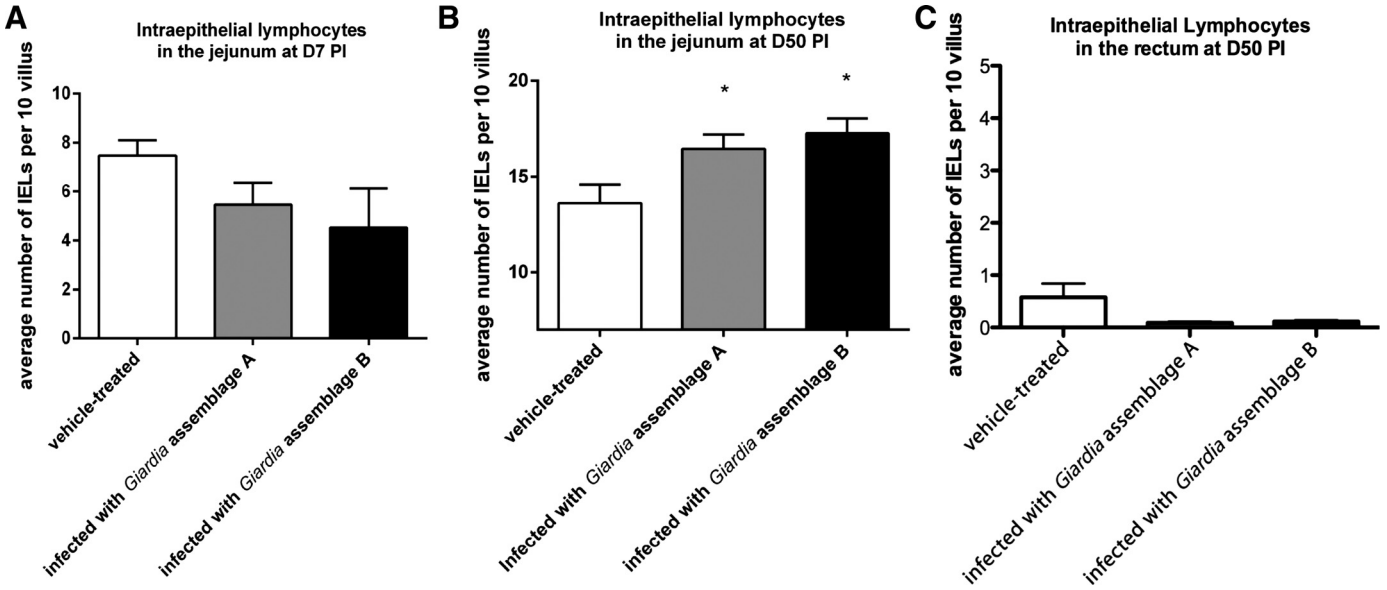

Fig. 3. *Giardia* induces an increase in intraepithelial lymphocytes (IELs) in the jejunum, but not in the rectum, of rats at 50 days PI with assemblage A or B: count of IELs in the jejunal mucosa of the vehicle-treated and *Giardia*-infected rats at 7 and 50 days PI after immunostaining with periodic acid-Schiff on 10 villi. *A* and *B*: average number of IELs per enterocyte in the jejunum of rats at 7 and 50 days PI. *C*: average number of IELs per enterocyte in the rectum of rats at 50 days PI. Values are means ± SE ($n = 10$ in each group). ****$P < 0.0001$ vs. vehicle-treated (by ANOVA and Tukey's test).

After 2, 3, and 6 h of incubation, while following similar patterns over the various time points, *E. coli* translocation was significantly increased ($P < 0.05$) in *G. duodenalis*- compared with vehicle-treated monolayers (Fig. 8). In an attempt to determine whether bacteria translocated via the transcellular route in a mechanism reminiscent of that recently observed in *C. jejuni* infection (42), a gentamicin assay was performed on Caco-2 cells grown to confluence exposed to *G. duodenalis* assemblage A and *E. coli* HB101. At the time of translocation, there were no significant differences in intracellular bacterial numbers between the cells treated with *E. coli* alone and those treated with both *Giardia* and *E. coli* (Fig. 9).

Additional experiments determined whether *Giardia*-induced bacterial translocation was associated with disruptions of the tight junction proteins occludin and claudin-4. We observed that *G. duodenalis* induces a reduction in occludin and claudin-4 protein levels in whole lysates at 1, 2, 3, and 6 h PI (Figs. 10 and 11).

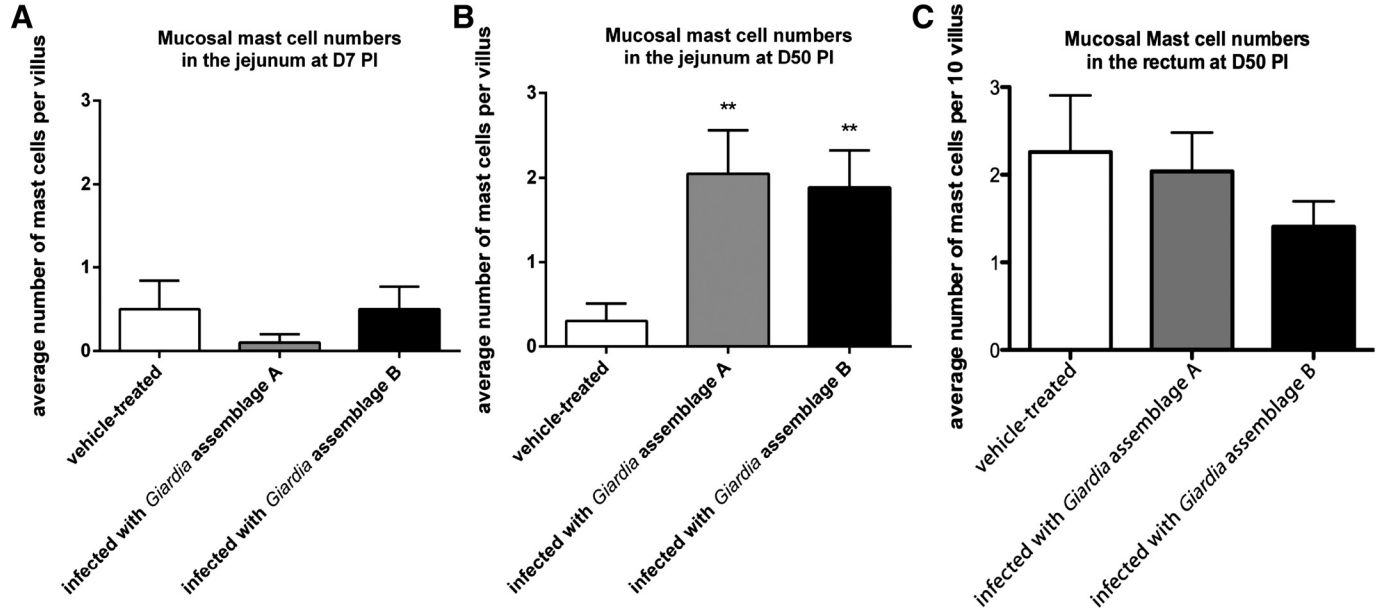

Fig. 4. *Giardia* induces mast cell infiltration in the jejunum, but not in the rectum, of rats at 50 days PI with assemblage A or B: count of mucosal mast cells after immunohistochemistry marking with a mast cell tryptase-directed antibody in the jejunum and rectum of control and *Giardia*-infected rats at 7 and 50 days PI on 100 villi. *A* and *B*: mucosal mast cell counts per villus in the jejunum of rats from each group (vehicle-treated, infected with assemblage A, and infected with assemblage B) at 7 and 50 days PI. *C*: mucosal mast cell counts per villus in the rectum of rats from each group at 50 days PI. Values are means ± SE ($n = 10$ in each group). **$P < 0.01$ vs. vehicle-treated (by ANOVA and Tukey's test).

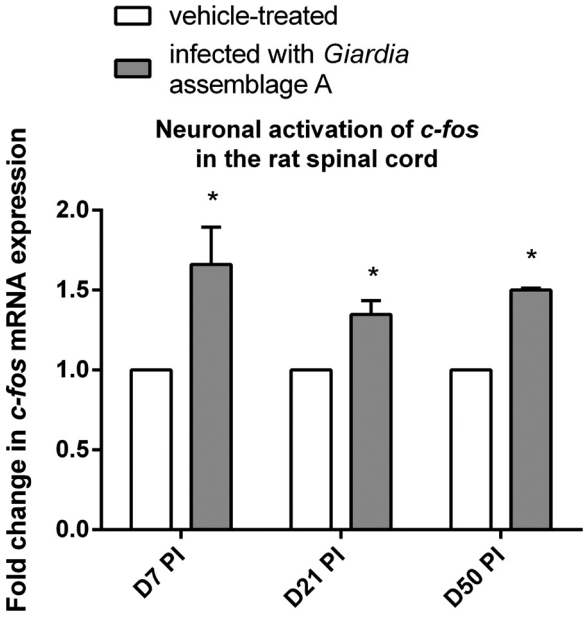

Fig. 5. Expression of *c-fos* mRNA in thoracolumbar spinal cord of *Giardia*-infected rats was significantly higher at 7, 21, and 50 days PI: expression of c-*fos* mRNA in thoracolumbar spinal cord segments of rats (control vs. *Giardia*-infected) at 7, 21, and 50 days PI. Values are means ± SE ($n = 10$ in each group). *$P < 0.05$ vs. vehicle-treated (by Student's *t*-test and Newman-Keuls test).

DISCUSSION

IBS may arise following acute enteritis with bacteria such as *E. coli, C. jejuni* (55, 77), and *Salmonella* spp. (58), viral enteropathogens (53), or parasites such as *Giardia* or *Cryptosporidium* (35, 46). A better understanding of the mechanisms by which this may occur is sorely warranted, and animal models for PI-IBS representative of the human pathology and using human pathogens are lacking. The recent outbreak in Bergen, Norway, underscored the significant potential of the parasite *G. duodenalis* to cause PI-IBS and lead to long-term GI symptoms. Using a novel *Giardia*-induced postinfectious model and in vitro mechanistic studies, the present study establishes, for the first time, a cause-and-effect relationship between giardiasis and postinfectious intestinal hypersensitivity with *Giardia* assemblage A or B. Consistent with clinical presentations in the human host, visceral hypersensitivity was observed in the small intestine as well as in the rectum, an area remote from any active colonization by the parasite. Hypersensitivity in the jejunum coincided with reduced VH, crypt hyperplasia, and increased mucosal IELs and mast cells. In the rectum, however, hypersensitivity could be measured in the absence of abnormal IEL or mast cell counts, again consistent with human presentations of PI-IBS that may occur in the presence of only mild inflammatory infiltration (2, 15). Starting in the acute phase of infection, *Giardia* facilitated the translocation of commensal bacteria and induced the expression of the protooncogene c-*fos*. Bacterial infiltration and c-*fos* expression were shown to persist in the postinfectious stage. In vitro findings indicate that *Giardia*-induced bacterial translocation is primarily paracellular, rather than transcellular, and implicate the degradation of tight junction proteins, including occludin and claudin-4.

Visceral hypersensitivity occurs in up to 80–90% of patients with IBS (60, 66) and has been reported throughout the GI tract, including the rectum (60), colon (27), jejunum (25), and

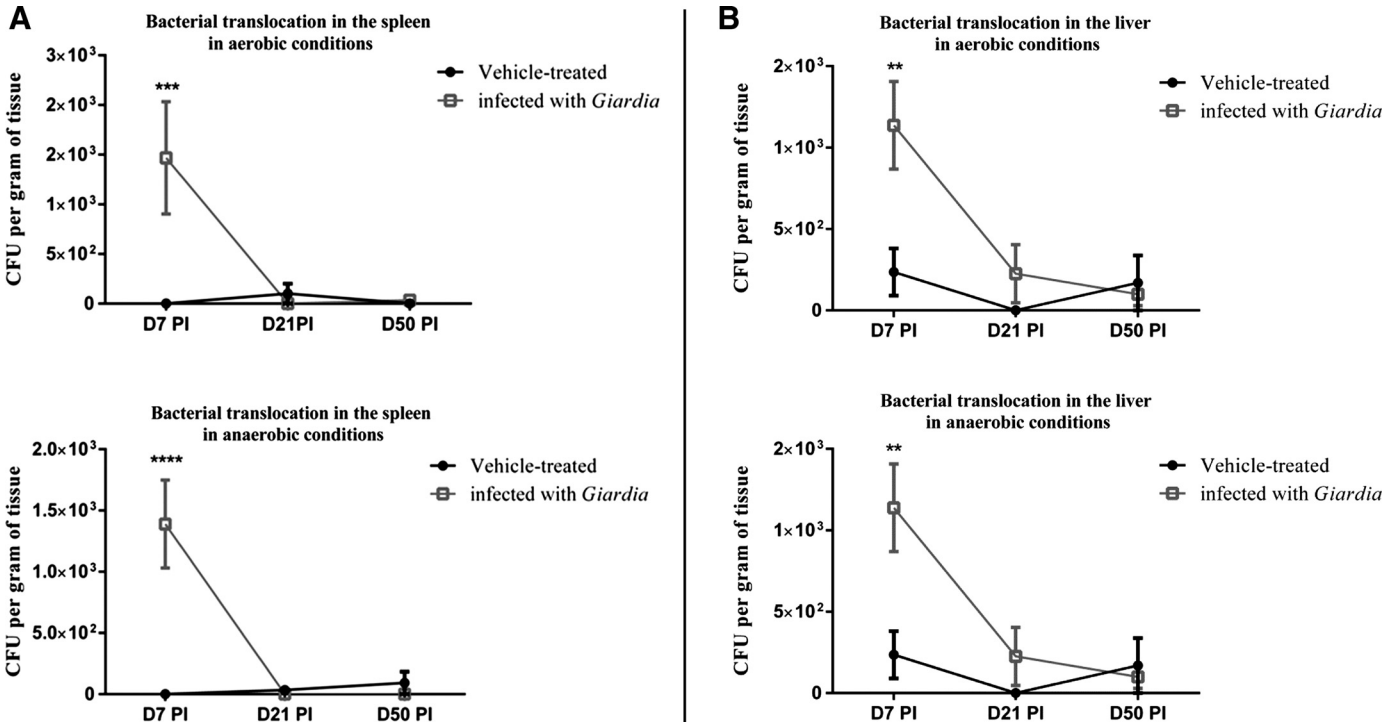

Fig. 6. *Giardia*-infected animals showed a significant translocation of commensal bacteria through the intestinal epithelium in liver and spleen during the acute stage of the disease: bacterial counts were examined in spleen and liver of vehicle-treated and *Giardia*-infected animals at 7, 21, and 50 days PI. *A* and *B*: bacterial translocation in spleen and liver at 7, 21, and 50 days PI in aerobic and anaerobic conditions. Values are means ± SE ($n = 5$ in each group at each time). **$P < 0.01$ and ***$P < 0.001$ vs. vehicle-treated (by Student's *t*-test and Newman-Keuls test).

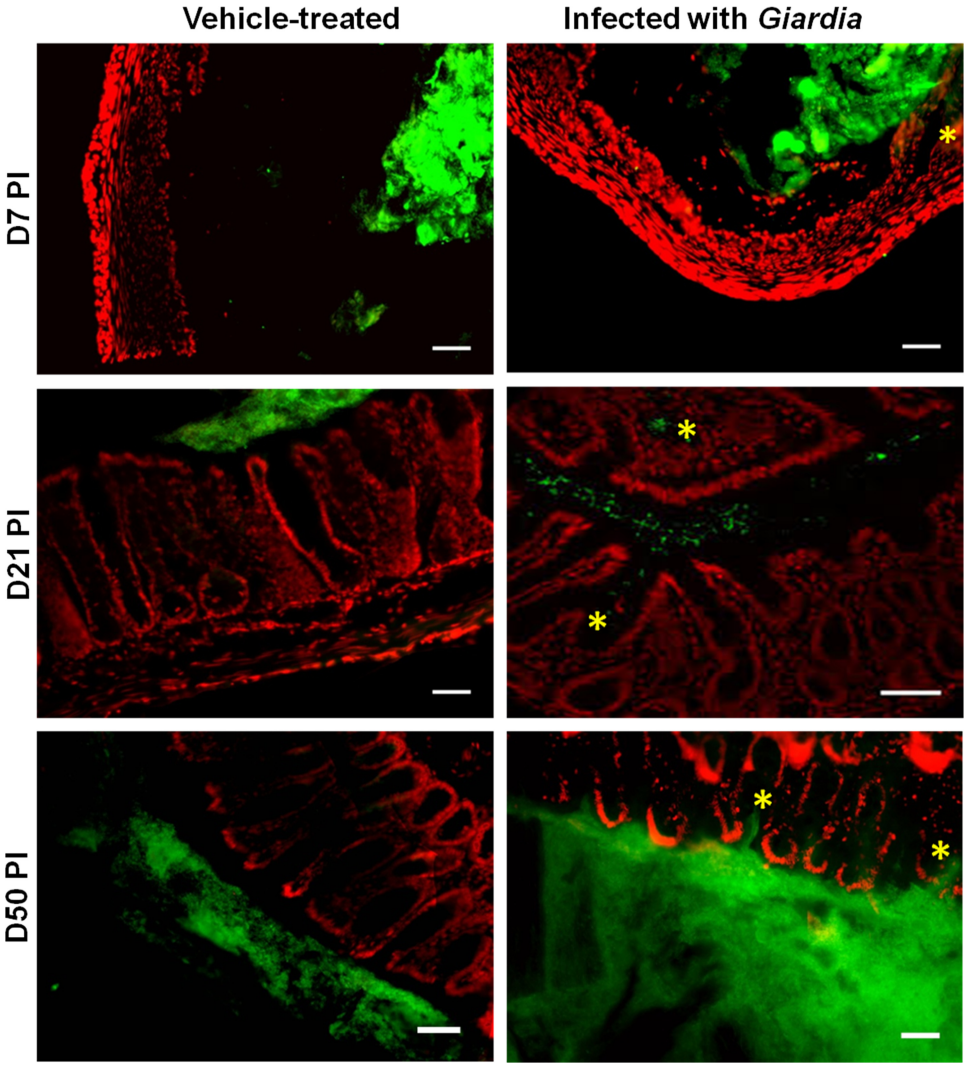

Fig. 7. Infiltration of commensal bacteria into the colonic mucosa during the infectious stages (7, 21, and 50 days PI): representative micrographs of bacterial infiltration into the rat colonic mucosa. All colonic segments were subjected to fluorescence in situ hybridization (FISH) with EUB338 probe, specific for the domain bacteria (16S rRNA). Bacteria were detected in the crypts, epithelial layer, and lamina propria of infected rats, but not in vehicle-treated animals. Host nuclei (4′,6-diamidino-2-phenylindole) stained red, and FISH-positive cells stained green (EUB338-Cy3). Scale bars = 50 μm, magnification ×200. Note bacterial infiltration in the mucosa (yellow asterisk) and microbiota in direct contact with the mucosa in *Giardia*-infected segment at 21 and 50 days PI.

esophagus (22). While both *Giardia* assemblages were able to cause hyperalgesia, allodynia appeared to be more marked with assemblage B. In 55% and 63% of rats infected with *Giardia* assemblages B and A, respectively, hypersensitivity developed at 50 days PI. In this model, while rats of both sexes were similarly represented in all groups, animals from either sex presented with postinfectious hypersensitivity (16 of 24 males and 7 of 8 females in the infected groups). Additional studies using this model system may help establish whether the degree of postinfectious visceral hypersensitivity following a transient infection with *G. duodenalis* may be sex-dependent (35). Indeed, some evidence indicates that sex differences in IBS symptoms may exist, particularly in industrialized countries, and female sex hormones may influence the severity of IBS (59).

In agreement with a number of previous reports, this study shows that different *Giardia* assemblages may cause different morphological modifications of the intestinal mucosa, depending on the time and site of the study (8, 17). Strain-dependent modifications of the mucosal morphology have been described in acute giardiasis in rats, as well as in other models, and in human subjects (12, 17). The present findings illustrate that villus atrophy may also occur at a time coinciding with postinfectious visceral hypersensitivity. In a number of intestinal disorders, including giardiasis, reduction in villus-to-crypt ratios correlates with impairments of digestion and absorption (12, 13). More research is needed to evaluate the role of the altered villus-crypt architecture in the development of IBS and its possible consequences for nutrient digestion and absorption at the time of visceral hypersensitivity, as postulated previously (26, 32).

IBS has been associated with increased numbers of mucosal mast cells and IELs in some studies and not in others (2, 5, 15). While the role of IELs in the pathophysiology of IBS remains unclear, mast cell tryptase and trypsin are well-established pathophysiological mediators of the activation of enteric cholinergic motor neurons and visceral pain in this disease (4, 5, 16). In addition, proteases combined with environmental factors, including stress, have been proposed to exacerbate visceral hypersensitivity after bacteria-induced colitis (38, 39). Previous research also demonstrated that mucosal, as well as connective tissue, mast cells were increased in giardiasis in association with increased molecular uptake by the mucosa (37). Consistent with these and other recent observations, the data reported here indicate that IEL and mast cell counts were increased in the jejunum of animals infected with *Giardia* of

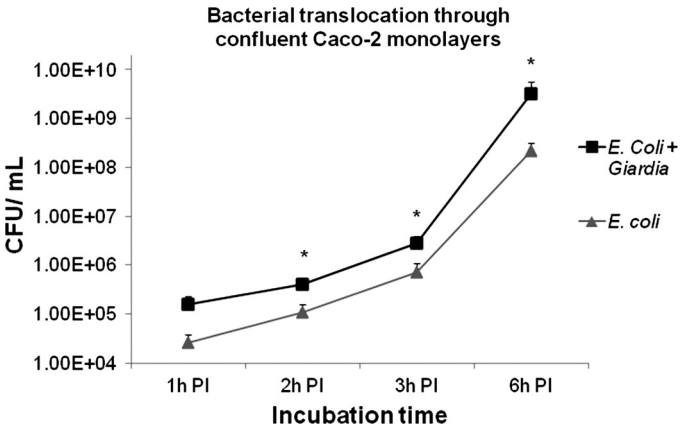

Fig. 8. *G. duodenalis* assemblage A facilitates the translocation of noninvasive *Escherichia coli* HB101 across confluent intestinal epithelial monolayers: translocation of a noninvasive *E. coli* HB101 through confluent Caco-2 monolayers on 3.0-μm-pore Transwell filter. Values represent the number of colony-forming units (CFUs) recovered from the basolateral compartment of the Transwell filter after incubation with *E. coli* HB101 alone or both *Giardia* and *E. coli* HB101 up to 6 h postexposure. Values are means ± SE of 4 independent experiments, where groups were tested in triplicate ($n = 9$ in each group). *$P < 0.05$ (by Student's *t*-test and Newman-Keuls test). Increase in bacterial translocation was significantly different in the presence of *Giardia* at 2, 3, and 6 h of incubation.

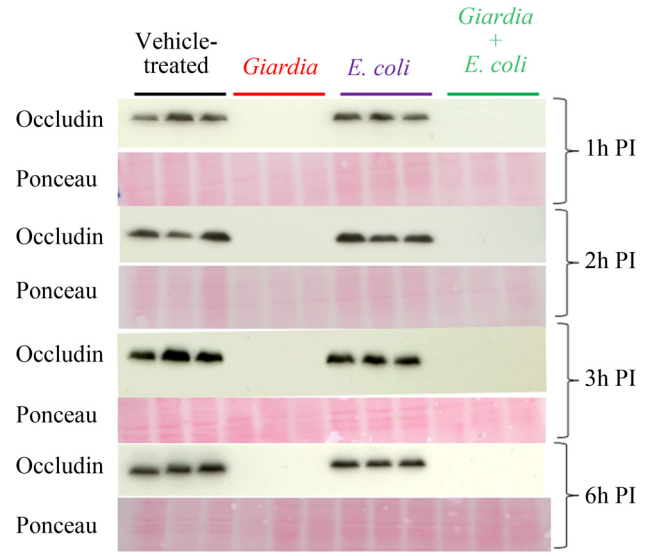

Fig. 10. *G. duodenalis* induces degradation of the tight junction protein occludin at 1, 2, 3, and 6 h postexposure: immunoblotting analysis of tight junction protein expression on standardized protein concentration (3 mg/ml). Ponceau red staining was used as loading control.

either assemblage, long after the parasite was cleared by the host (5, 31, 37, 46, 78). Elevated mucosal mast cell numbers have also been associated with increased levels of substance P and vasoactive intestinal peptide, both important mediators of diarrhea-predominant IBS in humans, as well as in rats (73). A recent report indicates that mast cells and nerve growth factor may play a key role in visceral hypersensitivity (80). Interestingly, however, the rectal hypersensitivity observed in our model did not correlate with IEL and mast cell hyperplasia. These observations are consistent with markers of IBS in patients in the presence or absence of inflammation (2, 5, 15). The findings reported here offer further support to the hypothesis that, while not absolutely required, elevated mast cell and IEL numbers in the mucosa may contribute to the pathophysiology of postgiardiasis IBS. Further studies using mast cell degranulation inhibitors or antagonists or mast cell stabilizers such compound 48/80 or doxantrazole, as described previously (49), will help confirm the role of mast cells in this model. In an attempt to further characterize the nociceptive signaling pathway involved in postgiardiasis visceral hypersensitivity, additional experiments assessed the expression of c-*fos*, a marker of nociceptive signaling known to be implicated in IBS (30, 82). The protein c-Fos is a nuclear transcription factor of genes involved in the adaptive response to painful stimuli (61). The results shown here demonstrate that c-*fos* expression is increased in the thoracolumbar section of the spinal cord in animals infected with *Giardia* during the acute stage of the disease (at 7 days), upon parasite clearance (at 21 days), and postinfectiously (at 50 days). Consistent with these findings,

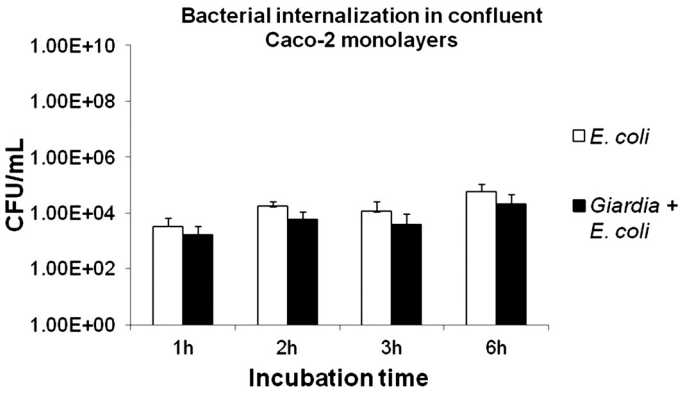

Fig. 9. *G. duodenalis* assemblage A does not induce *E. coli* HB101 internalization in confluent Caco-2 monolayers: internalization of a noninvasive *E. coli* HB101 in Caco-2 monolayers exposed to *E. coli* or *Giardia* + *E. coli* for up to 6 h. Values are means ± SE of 4 independent experiments, where each group was tested in triplicate. No significant difference was observed between *Giardia*- and *E. coli*-treated groups (by Student's *t*-test and Newman-Keuls test).

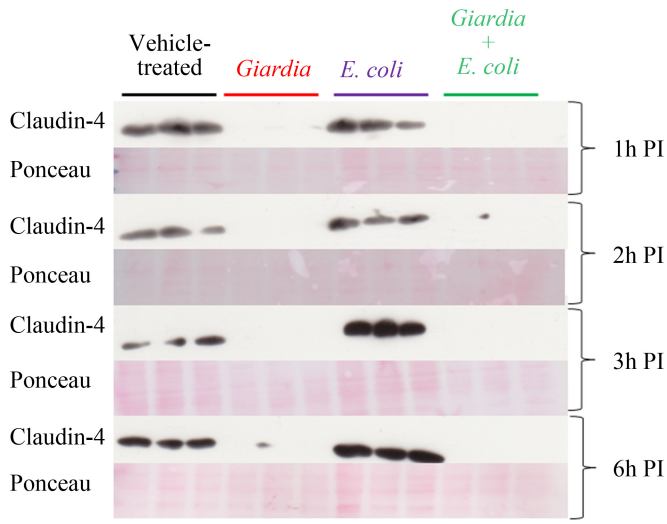

Fig. 11. *G. duodenalis* induces degradation of the tight junction protein claudin-4 at 1, 2, 3, and 6 h postexposure: immunoblotting analysis of tight junction protein expression on standardized protein concentration (3 mg/ml). Ponceau red staining was used as loading control.

intraperitoneal administration of a mast cell mediator has been found to activate c-*fos* in the dorsal horn neurons (48). Further research is needed to dissect the respective roles of mast cells and IELs in postinfectious visceral hypersensitivity, as proliferation of these immune cells appeared to be site-specific and to coincide with postinfectious c-*fos* expression, but not c-*fos* expression during the acute phase of the infection.

Another set of experiments further established whether postgiardiasis visceral hypersensitivity in this model was associated with other intestinal abnormalities linked to IBS in other studies. Intestinal microbiota play a key role in health and disease (72), and IBS has been associated with microbiota dysbiosis (21) and small intestinal bacterial overgrowth (62, 65). Moreover, we recently demonstrated that *Giardia* infection alters the host microbiota at a structural and a compositional level (6). Finally, numerous studies have also observed intestinal barrier dysfunction during IBS (63) and *Giardia* infection (18, 71). Results from the present experiments in vivo demonstrate that, indeed, *Giardia* induces the translocation of commensal bacteria during the acute stage of infection as well as postinfection, laying the foundations for other studies that will help identify pathogenic mechanisms of microbiota dysbiosis in PI-IBS. Indeed, bacterial translocation has been shown to trigger a macrophage-driven cytokine cascade that drives local inflammatory reaction and generates responses such as hyperalgesia and rectal hypersensitivity (20, 79). In addition, bacterial endotoxins have been shown to induce *fos* immunoreactivity (28). In the present experiments, FISH analysis revealed translocated bacteria in the infected colon, a site far from the active colonization by the parasitic trophozoites. FISH analysis also illustrated that the microbiota of *Giardia*-infected animals were closely apposed to the epithelial surface of the intestine, unlike those in vehicle-treated animals, where the commensal microorganisms were clearly separated from the host tissues by the space normally occupied by the host mucus lining. More research is warranted to determine whether and how *Giardia* may affect the intestinal mucus barrier and whether giardiasis may favor the development of mucolytic bacteria, as suggested in IBD (64).

Additional studies were performed in vitro in an attempt to characterize the mechanisms leading to the *Giardia*-induced loss of epithelial barrier function associated with postinfectious visceral hypersensitivity. Human colonic epithelial Caco-2 cell monolayers were exposed to *Giardia* assemblage A trophozoites with noninvasive *E. coli* HB101 meant to reflect what may happen to commensal bystanders during infection. *Giardia* promoted the translocation of noninvasive *E. coli* through the confluent epithelial monolayer. Short coincubation times of 2 h were sufficient for *Giardia* to induce the translocation of these bacteria. *Giardia* does not appear to induce internalization and subsequent transcellular passage of noninvasive *E. coli*, unlike the abnormalities induced by other enteropathogens such as *C. jejuni* (42).

Studies have shown that epithelial tight junctions are disrupted during IBS (10, 56), and *Giardia duodenalis* has been reported to degrade proteins of the apical junction complex such as zonula occludens-1, occludin, F-actin, α-actinin, E-cadherin, and claudin-1 (52, 71, 75). Consistent with these observations, the present results demonstrate that, indeed, increased bacterial translocation correlated with *G. duodenalis*-induced degradation of at least two transmembrane tight junction proteins, occludin and claudin-4, regardless of the presence or absence of noninvasive *E. coli*. Hence, this phenomenon can be caused by *Giardia* alone and does not require parasite interaction with commensal bacteria.

In conclusion, using a novel model system with the human enteropathogen *G. duodenalis*, we have established, for the first time, a cause-and-effect relationship between giardiasis and the development of postinfectious visceral hypersensitivity. This hypersensitivity occurred at the site of infection, as well as in areas of the GI tract such as the rectum, which is not colonized by the inciting enteropathogen, similar to hypersensitivity in patterns observed in human PI-IBS. Coinciding with *Giardia*-induced translocation of commensal bacteria during the acute and postinfectious stages of giardiasis, nociceptive c-*fos* is activated in the spinal dorsal horn. In association with these abnormalities, villus-crypt alterations and proliferation of mast cells and IELs could be detected in the jejunum, but not in the rectum. Finally, *Giardia*-induced translocation of commensal bacteria appears to favor the paracellular route, in conjunction with the degradation of the tight junction proteins occludin and claudin-4. Taken together, the findings point to key pathways whereby giardiasis may cause PI-IBS.

GRANTS

These studies were funded by the Natural Sciences and Engineering Research Council of Canada (Discovery and CREATE grant programs) and the French-Canada Collaborative Research Program. M. C. M. Halliez was sponsored by a French National Research Scholarship.

DISCLOSURES

No conflicts of interest, financial or otherwise, are declared by the authors.

AUTHOR CONTRIBUTIONS

M.C.M.H., J.-P.M., L.F., G. Gargala, T.K.L., C.A., and A.G.B. developed the concept and designed the research; M.C.M.H., T.D.F., G. Guerin, L.L., A.F., and E.C. performed the experiments; M.C.M.H., J.-P.M., and A.G.B. analyzed the data; M.C.M.H. interpreted the results of the experiments; M.C.M.H. prepared the figures; M.C.M.H. drafted the manuscript; M.C.M.H., J.-P.M., and A.G.B. edited and revised the manuscript; M.C.M.H., J.-P.M., T.D.F., L.L., A.F., L.F., G. Gargala, T.K.L., C.A., and A.G.B. approved the final version of the manuscript.

REFERENCES

1. **Arebi N, Gurmany S, Bullas D, Hobson A, Stagg A, Kamm M.** The psychoneuroimmunology of irritable bowel syndrome—an exploration of interactions between psychological, neurological and immunological observations. *Aliment Pharmacol Ther* 28: 830–840, 2008.
2. **Arévalo F, Aragon V, Montes P, Guzmán E, Monge E.** [Increase of intraepithelial lymphocytes in patients with irritable bowel syndrome]. *Rev Gastroenterol Perú* 31: 315–318, 2011.
3. **Azpiroz F, Bouin M, Camilleri M, Mayer EA, Poitras P, Serra J, Spiller RC.** Mechanisms of hypersensitivity in IBS and functional disorders. *Neurogastroenterol Motil* 19: 62–88, 2007.
4. **Balestra B, Vicini R, Cremon C, Zecchi L, Dothel G, Vasina V, De Giorgio R, Paccapelo A, Pastoris O, Stanghellini V, Corinaldesi R, De Ponti F, Tonini M, Barbara G.** Colonic mucosal mediators from patients with irritable bowel syndrome excite enteric cholinergic motor neurons. *Neurogastroenterol Motil* 24: 1118–e570, 2012.
5. **Barbara G, Stanghellini V, De Giorgio R, Cremon C, Cottrell GS, Santini D, Pasquinelli G, Morselli-Labate AM, Grady EF, Bunnett NW, Collins SM, Corinaldesi R.** Activated mast cells in proximity to colonic nerves correlate with abdominal pain in irritable bowel syndrome. *Gastroenterology* 126: 693–702, 2004.
6. **Beatty JK, Akierman S, Rioux K, Beck P, McKnight W, Feener T, Wallace J, Buret A.** Gut microbiota biofilm disruptions by *Giardia*: pathology in human enterocytes and germ-free mice (Abstract). *FASEB J* 27: 131.1, 2013.

7. **Beatty JK, Bhargava A, Buret AG.** Post-infectious irritable bowel syndrome: mechanistic insights into chronic disturbances following enteric infection. *World J Gastroenterol* 20: 3976–3985, 2014.
8. **Bénéré E, Van Assche T, Van Ginneken C, Peulen O, Cos P, Maes L.** Intestinal growth and pathology of *Giardia duodenalis* assemblage subtype A_I, A_{II}, B and E in the gerbil model. *Parasitology* 139: 424–433, 2012.
9. **Bercík P, Wang L, Verdú EF, Mao YK, Blennerhassett P, Khan WI, Kean I, Tougas G, Collins SM.** Visceral hyperalgesia and intestinal dysmotility in a mouse model of postinfective gut dysfunction. *Gastroenterology* 127: 179–187, 2004.
10. **Bertiaux-Vandaële N, Youmba SB, Belmonte L, Lecleire S, Antonietti M, Gourcerol G, Leroi AM, Déchelotte P, Ménard JF, Ducrotté P, Coëffier M.** The expression and the cellular distribution of the tight junction proteins are altered in irritable bowel syndrome patients with differences according to the disease subtype. *Am J Gastroenterol* 106: 2165–2173, 2011.
11. **Buret A, denHollander N, Wallis PM, Befus D, Olson ME.** Zoonotic potential of giardiasis in domestic ruminants. *J Infect Dis* 162: 231–237, 1990.
12. **Buret A, Gall DG, Olson ME.** Effects of murine giardiasis on growth, intestinal morphology, and disaccharidase activity. *J Parasitol* 76: 403–409, 1990.
13. **Buret A, Gall DG, Olson ME.** Growth, activities of enzymes in the small intestine, and ultrastructure of microvillous border in gerbils infected with *Giardia duodenalis*. *Parasitol Res* 77: 109–114, 1991.
14. **Buret A, Hardin JA, Olson ME, Gall DG.** Pathophysiology of small intestinal malabsorption in gerbils infected with *Giardia lamblia*. *Gastroenterology* 103: 506–513, 1992.
15. **Camilleri M, Lasch K, Zhou W.** Irritable bowel syndrome: methods, mechanisms, and pathophysiology. The confluence of increased permeability, inflammation, and pain in irritable bowel syndrome. *Am J Physiol Gastrointest Liver Physiol* 303: G775–G785, 2012.
16. **Cenac N, Andrews CN, Holzhausen M, Chapman K, Cottrell G, Andrade-Gordon P, Steinhoff M, Barbara G, Beck P, Bunnett NW, Sharkey KA, Ferraz JG, Shaffer E, Vergnolle N.** Role for protease activity in visceral pain in irritable bowel syndrome. *J Clin Invest* 117: 636–647, 2007.
17. **Cevallos A, Carnaby S, James M, Farthing JG.** Small intestinal injury in a neonatal rat model of giardiasis is strain dependent. *Gastroenterology* 109: 766–773, 1995.
18. **Chen TL, Chen S, Wu HW, Lee TC, Lu YZ, Wu LL, Ni YH, Sun CH, Yu WH, Buret AG, Yu LC.** Persistent gut barrier damage and commensal bacterial influx following eradication of *Giardia* infection in mice. *Gut Pathog* 5: 26, 2013.
19. **Clarke G, Quigley EM, Cryan JF, Dinan TG.** Irritable bowel syndrome: towards biomarker identification. *Trends Mol Med* 15: 478–489, 2009.
20. **Coelho AM, Fioramonti J, Buéno L.** Systemic lipopolysaccharide influences rectal sensitivity in rats: role of mast cells, cytokines, and vagus nerve. *Am J Physiol Gastrointest Liver Physiol* 279: G781–G790, 2000.
21. **Collins SM.** A role for the gut microbiota in IBS. *Nat Rev Gastroenterol* 11: 497–505, 2014.
22. **Costantini M, Sturniolo GC, Zaninotto G, D'Incà R, Polo R, Naccarato R, Ancona E.** Altered esophageal pain threshold in irritable bowel syndrome. *Dig Dis Sci* 38: 206–212, 1993.
23. **Cotton JA, Beatty JK, Buret AG.** Host parasite interactions and pathophysiology in *Giardia* infections. *Int J Parasitol* 41: 925–933, 2011.
24. **Diamond LS, Harlow DR, Cunnick CC.** A new medium for the axenic cultivation of *Entamoeba histolytica* and other *Entamoeba*. *Trans R Soc Trop Med Hyg* 72: 431–432, 1978.
25. **Evans PR, Bennett EJ, Bak YT, Tennant CC, Kellow JE.** Jejunal sensorimotor dysfunction in irritable bowel syndrome: clinical and psychosocial features. *Gastroenterology* 110: 393–404, 1996.
26. **Evans PR, Piesse C, Bak YT, Kellow JE.** Fructose-sorbitol malabsorption and symptom provocation in irritable bowel syndrome: relationship to enteric hypersensitivity and dysmotility. *Scand J Gastroenterol* 33: 1158–1163, 1998.
27. **Fent J, Balázs L, Buzás G, Erasmus LP, Hölzl R, Kovács A, Weisz J, Adám G.** Colonic sensitivity in irritable bowel syndrome and normal subjects according to their hemispheric preference and cognitive style. *Integr Physiol Behav Sci* 34: 54–62, 1999.
28. **Gaykema RP, Goehler LE, Tilders FJ, Bol JG, McGorry M, Fleshner M, Maier SF, Watkins LR.** Bacterial endotoxin induces fos immunoreactivity in primary afferent neurons of the vagus nerve. *Neuroimmunomodulation* 5: 234–240, 1998.
29. **Geurden T, Geldhof P, Levecke B, Martens C, Berkvens D, Casaert S, Vercruysse J, Claerebout E.** Mixed *Giardia duodenalis* assemblage A and E infections in calves. *Int J Parasitol* 38: 259–264, 2008.
30. **Gibney SM, Gosselin RD, Dinan TG, Cryan JF.** Colorectal distension-induced prefrontal cortex activation in the Wistar-Kyoto rat: implications for irritable bowel syndrome. *Neuroscience* 165: 675–683, 2010.
31. **Gillon J, Al Thamery D, Ferguson A.** Features of small intestinal pathology (epithelial cell kinetics, intraepithelial lymphocytes, disaccharidases) in a primary *Giardia muris* infection. *Gut* 23: 498–506, 1982.
32. **Goldstein R, Braverman D, Stankiewicz H.** Carbohydrate malabsorption and the effect of dietary restriction on symptoms of irritable bowel syndrome and functional bowel complaints. *Isr Med Assoc J* 2: 583–587, 2000.
33. **Halliez MC, Buret AG.** Extra-intestinal and long term consequences of *Giardia duodenalis* infections. *World J Gastroenterol* 19: 8974–8985, 2013.
34. **Halvorson HA, Schlett CD, Riddle MS.** Postinfectious irritable bowel syndrome—a meta-analysis. *Am J Gastroenterol* 101: 1894–1899; quiz 1942, 2006.
35. **Hanevik K, Dizdar V, Langeland N, Hausken T.** Development of functional gastrointestinal disorders after *Giardia lamblia* infection. *BMC Gastroenterol* 9: 27, 2009.
36. **Hanevik K, Wensaas KA, Rortveit G, Eide GE, Mørch K, Langeland N.** Irritable bowel syndrome and chronic fatigue 6 years after *Giardia* infection: a controlled prospective cohort study. *Clin Infect Dis* 59: 1394–1400, 2014.
37. **Hardin JA, Buret AG, Olson ME, Kimm MH, Gall DG.** Mast cell hyperplasia and increased macromolecular uptake in an animal model of giardiasis. *J Parasitol* 83: 908–912, 1997.
38. **Ibeakanma C, Ochoa-Cortes F, Miranda-Morales M, McDonald T, Spreadbury I, Cenac N, Cattaruzza F, Hurlbut D, Vanner S, Bunnett N, Vergnolle N, Vanner S.** Brain-gut interactions increase peripheral nociceptive signaling in mice with postinfectious irritable bowel syndrome. *Gastroenterology* 141: 2098–2108, 2011.
39. **Jacobson K, McHugh K, Collins S.** The mechanism of altered neural function in a rat model of acute colitis. *Gastroenterology* 112: 156–162, 1997.
40. **Jawed H, Jamall S, Shah SU, Perveen K, Hanif F, Simjee SU.** *N*-(2-hydroxy phenyl) acetamide produces profound inhibition of c-Fos protein and mRNA expression in the brain of adjuvant-induced arthritic rats. *Mol Cell Biochem* 387: 81–90, 2014.
41. **Jones R, Lydeard S.** Irritable bowel syndrome in the general population. *BMJ* 304: 87–90, 1992.
42. **Kalischuk LD, Inglis GD, Buret AG.** *Campylobacter jejuni* induces transcellular translocation of commensal bacteria via lipid rafts. *Gut Pathog* 1: 2, 2009.
43. **Kassinen A, Krogius-Kurikka L, Mäkivuokko H, Rinttilä T, Paulin L, Corander J, Malinen E, Apajalahti J, Palva A.** The fecal microbiota of irritable bowel syndrome patients differs significantly from that of healthy subjects. *Gastroenterology* 133: 24–33, 2007.
44. **Keister DB.** Axenic culture of *Giardia lamblia* in TYI-S-33 medium supplemented with bile. *Trans R Soc Trop Med Hyg* 77: 487–488, 1983.
45. **Kellow JE, Phillips SF, Miller LJ, Zinsmeister AR.** Dysmotility of the small intestine in irritable bowel syndrome. *Gut* 29: 1236–1243, 1988.
46. **Khaldi S, Gargala G, Le Goff L, Parey S, Francois A, Fioramonti J, Ballet JJ, Dupont JP, Ducrotté P, Favennec L.** *Cryptosporidium parvum* isolate-dependent postinfectious jejunal hypersensitivity and mast cell accumulation in an immunocompetent rat model. *Infect Immun* 77: 5163–5169, 2009.
47. **Levecke B, Geldhof P, Claerebout E, Dorny P, Vercammen F, Cacciò SM, Vercruysse J, Geurden T.** Molecular characterisation of *Giardia duodenalis* in captive non-human primates reveals mixed assemblage A and B infections and novel polymorphisms. *Int J Parasitol* 39: 1595–1601, 2009.
48. **Levy D, Kainz V, Burstein R, Strassman AM.** Mast cell degranulation distinctly activates trigemino-cervical and lumbosacral pain pathways and elicits widespread tactile pain hypersensitivity. *Brain Behav Immun* 26: 311–317, 2012.
49. **Li E, Zhao A, Shea-Donohue T, Singer SM.** Mast cell-mediated changes in smooth muscle contractility during mouse giardiasis. *Infect Immun* 75: 4514–4518, 2007.

50. **Li WM, Suzuki A, Cui KM.** Responses of blood pressure and renal sympathetic nerve activity to colorectal distension in anesthetized rats. *J Physiol Sci* 56: 153–156, 2006.
51. **Lovell RM, Ford AC.** Global prevalence of and risk factors for irritable bowel syndrome: a meta-analysis. *Clin Gastroenterol Hepatol* 10: 712–721, 2012.
52. **Maia-Brigagão C, Morgado-Díaz JA, De Souza W.** *Giardia* disrupts the arrangement of tight, adherens and desmosomal junction proteins of intestinal cells. *Parasitol Int* 61: 280–287, 2012.
53. **Marshall JK, Thabane M, Borgaonkar MR, James C.** Postinfectious irritable bowel syndrome after a food-borne outbreak of acute gastroenteritis attributed to a viral pathogen. *Clin Gastroenterol Hepatol* 5: 457–460, 2007.
54. **Marshall JK, Thabane M, Garg AX, Clark WF, Moayyedi P, Collins SM, Walkerton Health Study Investigators.** Eight year prognosis of postinfectious irritable bowel syndrome following waterborne bacterial dysentery. *Gut* 59: 605–611, 2010.
55. **Marshall JK, Thabane M, Garg AX, Clark WF, Salvadori M, Collins SM, Walkerton Health Study Investigators.** Incidence and epidemiology of irritable bowel syndrome after a large waterborne outbreak of bacterial dysentery. *Gastroenterology* 131: 445–450, 2006.
56. **Martínez C, Vicario M, Ramos L, Lobo B, Mosquera JL, Alonso C, Sánchez A, Guilarte M, Antolín M, de Torres I, González-Castro AM, Pigrau M, Saperas E, Azpiroz F, Santos J.** The jejunum of diarrhea-predominant irritable bowel syndrome shows molecular alterations in the tight junction signaling pathway that are associated with mucosal pathobiology and clinical manifestations. *Am J Gastroenterol* 107: 736–746, 2012.
57. **McLean PG, Picard C, Garcia-Villar R, Moré J, Fioramonti J, Buéno L.** Effects of nematode infection on sensitivity to intestinal distension: role of tachykinin NK2 receptors. *Eur J Pharmacol* 337: 279–282, 1997.
58. **Mearin F, Pérez-Oliveras M, Perelló A, Vinyet J, Ibañez A, Coderch J, Perona M.** Dyspepsia and irritable bowel syndrome after a *Salmonella gastroenteritis* outbreak: one-year follow-up cohort study. *Gastroenterology* 129: 98–104, 2005.
59. **Meleine M, Matricon J.** Gender-related differences in irritable bowel syndrome: potential mechanisms of sex hormones. *World J Gastroenterol* 20: 6725–6743, 2014.
60. **Mertz H, Naliboff B, Munakata J, Niazi N, Mayer EA.** Altered rectal perception is a biological marker of patients with irritable bowel syndrome. *Gastroenterology* 109: 40–52, 1995.
61. **Morgan JI, Curran T.** Inducible proto-oncogenes of the nervous system: their contribution to transcription factors and neuroplasticity. *Prog Brain Res* 86: 287–294, 1990.
62. **O'Leary C, Quigley EM.** Small bowel bacterial overgrowth, celiac disease, and IBS: what are the real associations? *Am J Gastroenterol* 98: 720–722, 2003.
63. **Piche T, Barbara G, Aubert P, Bruley des Varannes S, Dainese R, Nano JL, Cremon C, Stanghellini V, De Giorgio R, Galmiche JP, Neunlist M.** Impaired intestinal barrier integrity in the colon of patients with irritable bowel syndrome: involvement of soluble mediators. *Gut* 58: 196–201, 2009.
64. **Png CW, Lindén SK, Gilshenan KS, Zoetendal EG, McSweeney CS, Sly LI, McGuckin MA, Florin TH.** Mucolytic bacteria with increased prevalence in IBD mucosa augment in vitro utilization of mucin by other bacteria. *Am J Gastroenterol* 105: 2420–2428, 2010.
65. **Posserud I, Stotzer PO, Björnsson ES, Abrahamsson H, Simrén M.** Small intestinal bacterial overgrowth in patients with irritable bowel syndrome. *Gut* 56: 802–808, 2007.
66. **Ritchie J.** Pain from distension of the pelvic colon by inflating a balloon in the irritable colon syndrome. *Gut* 14: 125–132, 1973.
67. **Romero-Calvo I, Ocón B, Martínez-Moya P, Suárez MD, Zarzuelo A, Martínez-Augustin O, de Medina FS.** Reversible Ponceau staining as a loading control alternative to actin in Western blots. *Anal Biochem* 401: 318–320, 2010.
68. **Roxström-Lindquist K, Palm D, Reiner D, Ringqvist E, Svärd SG.** *Giardia* immunity—an update. *Trends Parasitol* 22: 26–31, 2006.
69. **Saleh TM, Connell BJ, Allen GV.** Visceral afferent activation-induced changes in sympathetic nerve activity and baroreflex sensitivity. *Am J Physiol Regul Integr Comp Physiol* 276: R1780–R1791, 1999.
70. **Schmittgen TD, Livak KJ.** Analyzing real-time PCR data by the comparative C_T method. *Nat Protoc* 3: 1101–1108, 2008.
71. **Scott KG, Meddings JB, Kirk DR, Lees-Miller SP, Buret AG.** Intestinal infection with *Giardia* spp. reduces epithelial barrier function in a myosin light chain kinase-dependent fashion. *Gastroenterology* 123: 1179–1190, 2002.
72. **Sekirov I, Russell SL, Antunes LC, Finlay BB.** Gut microbiota in health and disease. *Physiol Rev* 90: 859–904, 2010.
73. **Sohn W, Lee OY, Lee SP, Lee KN, Jun DW, Lee HL, Yoon BC, Choi HS, Sim J, Jang KS.** Mast cell number, substance P and vasoactive intestinal peptide in irritable bowel syndrome with diarrhea. *Scand J Gastroenterol* 49: 43–51, 2014.
74. **Sundin J, Rangel I, Kumawat AK, Hultgren-Hörnquist E, Brummer RJ.** Aberrant mucosal lymphocyte number and subsets in the colon of post-infectious irritable bowel syndrome patients. *Scand J Gastroenterol* 49: 1068–1075, 2014.
75. **Teoh DA, Kamieniecki D, Pang G, Buret AG.** *Giardia lamblia* rearranges F-actin and α-actinin in human colonic and duodenal monolayers and reduces transepithelial electrical resistance. *J Parasitol* 86: 800–806, 2000.
76. **Thabane M, Kottachchi DT, Marshall JK.** Systematic review and meta-analysis: the incidence and prognosis of post-infectious irritable bowel syndrome. *Aliment Pharmacol Ther* 26: 535–544, 2007.
77. **Thabane M, Simunovic M, Akhtar-Danesh N, Garg AX, Clark WF, Collins SM, Salvadori M, Marshall JK.** An outbreak of acute bacterial gastroenteritis is associated with an increased incidence of irritable bowel syndrome in children. *Am J Gastroenterol* 105: 933–939, 2010.
78. **Walker MM, Talley NJ, Prabhakar M, Pennaneac'h CJ, Aro P, Ronkainen J, Storskrubb T, Harmsen WS, Zinsmeister AR, Agreus L.** Duodenal mastocytosis, eosinophilia and intraepithelial lymphocytosis as possible disease markers in the irritable bowel syndrome and functional dyspepsia. *Aliment Pharmacol Ther* 29: 765–773, 2009.
79. **Wang B, Glatzle J, Mueller MH, Kreis M, Enck P, Grundy D.** Lipopolysaccharide-induced changes in mesenteric afferent sensitivity of rat jejunum in vitro: role of prostaglandins. *Am J Physiol Gastrointest Liver Physiol* 289: G254–G260, 2005.
80. **Willot S, Gauthier C, Patey N, Faure C.** Nerve growth factor content is increased in the rectal mucosa of children with diarrhea-predominant irritable bowel syndrome. *Neurogastroenterol Motil* 24: 734–739, e347, 2012.
81. **World Health Organization.** *Guidelines for Drinking-Water Quality — Volume 1: Recommendations* (3rd ed., incorporating first and second addenda). Geneva: World Health Organization, 2008. http://www.who.int/water_sanitation_health/dwq/gdwq3/en/.
82. **Zhang R, Zou N, Li J, Lv H, Wei J, Fang XC, Qian JM.** Elevated expression of c-*fos* in central nervous system correlates with visceral hypersensitivity in irritable bowel syndrome (IBS): a new target for IBS treatment. *Int J Colorectal Dis* 26: 1035–1044, 2011.